



## Diffuse X-ray Scattering from Optically Pure Ibuprofen

P.A. Altin<sup>a</sup> and D.J. Goossens<sup>b</sup>

<sup>a</sup> *Department of Physics, Australian National University, Canberra 0200, Australia.*

<sup>b</sup> *Research School of Chemistry, Australian National University, Canberra 0200, Australia.*

The crystal structure of optically pure Ibuprofen ('S+ibuprofen') has been studied through diffuse x-ray scattering. Data from a single crystal were compared with calculated patterns using a model crystal placed in thermal equilibrium using a Monte Carlo (MC) algorithm. We present some preliminary results from analysis and interpretation of the structured diffuse scattering.

### 1. Introduction

Diffuse scattering, the weak background between sharp Bragg peaks in an x-ray diffraction pattern, arises due to deviations from the ideal crystal lattice, often due to thermal motion. Correlations in these displacements, which reflect the flexibility and interactions of molecules in the lattice environment, affect the pattern of diffuse scattering observed from a sample [1]. Studying these interactions through diffuse scattering can provide insight into the conformational behaviour of polymorphic pharmaceuticals.

In this work, x-ray scattering data was collected at room temperature from crystals of S+ibuprofen. A model crystal was constructed based on the known average crystal structure and placed in thermal equilibrium using a MC simulation. Inter- and intra-molecular interactions were modelled by simple harmonic potentials with variable force constants. Computed scattering patterns were compared to the experimental data to isolate key features of the model.

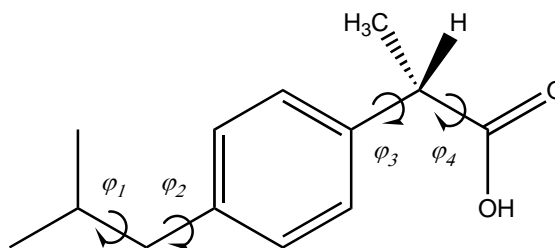


Fig. 1. S+ibuprofen. Rotation (modelled by torsional springs) is permitted about the four single bonds marked, giving four internal degrees of freedom  $\varphi_i$ .

### 2. Experimental

S+ibuprofen single crystals were grown by slow evaporation from n-hexane and by temperature change ( $40^\circ\text{C}$  to  $10^\circ\text{C}$  at  $5\text{Kd}^{-1}$ ) in acetonitrile. Diffuse scattering data were collected using a mar345 image plate area detector and  $17.5\text{ keV}$  ( $\lambda = 0.71069\text{ \AA}$ ) Mo  $K\alpha$  x-rays. Reciprocal space planes were extracted from the raw data and processed to remove artefacts [2]. Fig. 2 shows diffuse scattering in the  $h1l$ ,  $hk0$  and a  $101$  plane.

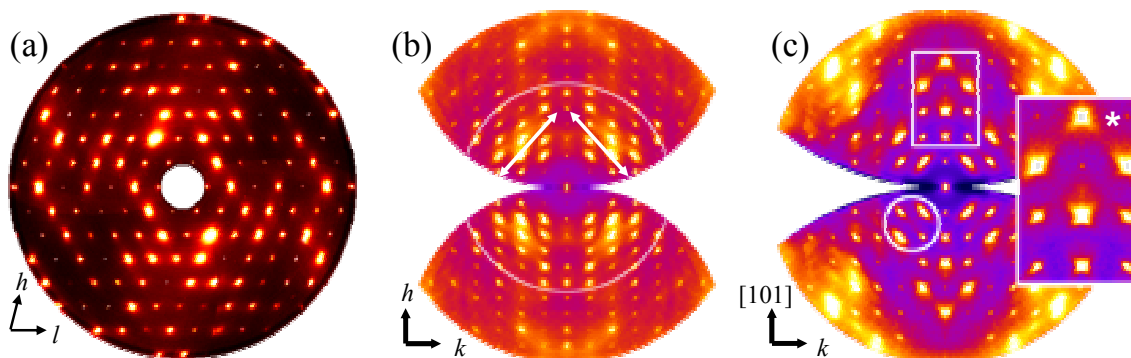


Fig. 2. Diffuse scattering in the (a)  $h1l$ , (b)  $hk0$  and (c)  $101$  planes. The circle in (b) indicates the section of the plane calculated from the model (Fig. 4). False colour palettes have been applied.



### 3. The Model Crystal

A network of contact vectors describes the intermolecular interactions in the model crystal. Each contact is treated as an ideal spring. A harmonic energy is also associated with torsional rotation of the bonds marked in Fig. 1, giving:

$$E_{total} = E_{inter} + E_{intra} = \sum_{\substack{\text{contact} \\ \text{vectors}}} \kappa_i (d_i - d_{0i})^2 + \sum_{\text{molecules}} \left( \sum_i \kappa_i^* (\Delta\varphi_i)^2 \right)$$

where  $\kappa$  and  $\kappa^*$  are the force constants,  $(d - d_0)$  is the displacement of each contact from its equilibrium length, and  $\Delta\varphi$  is the change in torsional angle. The lattice parameters applied were:  $a = 12.456(4)$  Å,  $b = 8.0362(11)$  Å,  $c = 13.533(3)$  Å and  $\beta = 112.86(2)^\circ$  [3]. A Metropolis Monte Carlo algorithm was used to bring the model crystal into thermal equilibrium [4]. Diffraction patterns were then calculated from the correlated equilibrium structure. Bragg peaks were subtracted to make the diffuse scattering more apparent.

### 4. Results and Analysis

#### 4.1 Isotropic intermolecular contacts:

A simple model with all intermolecular spring constants equal and no torsional rotation allowed reproduced the scattering in the  $h0l$  and  $h1l$  planes well (see Fig. 3). This suggests that correlations in these planes are isotropic as there seems to be no dominant interaction. However, this basic model failed to recreate key features of the  $hk0$  plane, particularly the lengthening of diffuse spots along the diagonal (marked with arrows in Fig. 2).

#### 4.2 Torsional rotation model:

This model was then adjusted to allow bond rotation. With the torsional spring constants  $k_i^*$  set to zero (such that  $E_{intra} \ll E_{inter}$ ), the fit of the  $h0l$  and  $h1l$  planes to the experimental data was improved, and the expected stretching of diffuse spots in the  $hk0$  plane (Fig. 4) was observed. The agreement of this calculation with the experimental data suggests that quite unhindered torsional rotation is important in the S+ibuprofen crystal, with significantly less energy in such motion than in the intermolecular interactions.

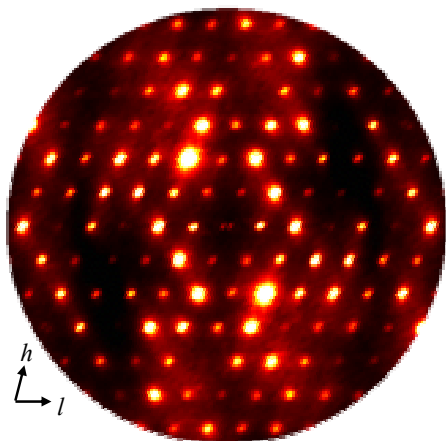


Fig. 3. Calculated diffuse scattering in the  $h1l$  plane with all spring constants equal. Compare with Fig. 2 (a).

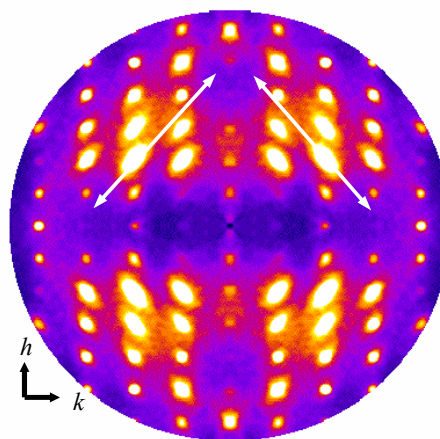


Fig. 4. Calculated diffuse scattering in the  $hk0$  plane with torsional spring constants set to zero. Compare with the inner part of Fig. 3 (c).



#### 4.3 Dimerising hydrogen bonding interaction:

It was expected that the strongest intermolecular interaction in the S+ibuprofen crystal would be the dimerising -COOH—HOOC- hydrogen bond, as recently found to be the case in the racemate [5]. Initial analysis of the experimental data appears to support this, with diffuse features stretched more in the 101 plane (Fig. 2c) where the direction of this interaction coincides with the molecular axis. This forms chains of molecules (Fig. 5) which collapse diffuse scattering into characteristic stretched lines. In addition, several box-shaped features are seen along the vertical axis (marked with an asterisk in Fig. 2c). These also suggest strong correlations at  $\sim 45^\circ$  to the horizontal. A model with these H-bond contacts strengthened 100-fold (Fig. 6) reproduced the elongation and these box-shaped figures.

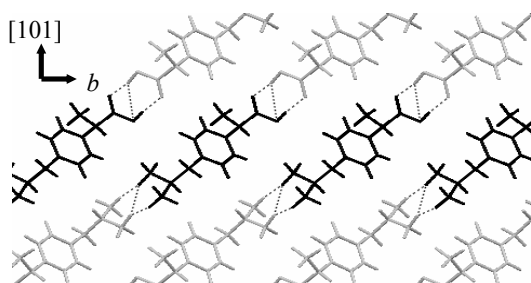


Fig. 5. A section of the crystal as seen along the  $[-101]$  direction, showing as dashed lines the dimerising hydrogen bonding interactions running at  $\sim 45^\circ$  to the horizontal.

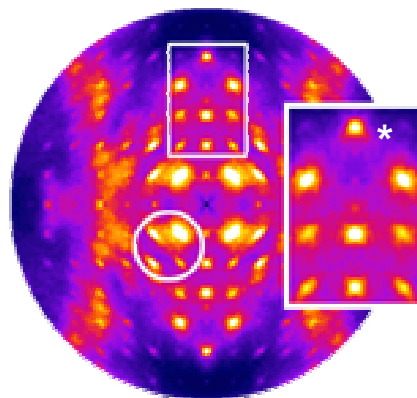


Fig. 6. Calculated diffuse scattering in the 101 plane with H-bond contacts strengthened by a factor of 100. Compare with Fig. 2(c).

Although the calculated pattern in this plane is not a precise reproduction of the diffuse scattering data, the presence of some corresponding attributes is evident. In particular, the scattering figures magnified in the inset in Fig. 6 successfully recreate the equivalent section of the experimental data (Fig. 2c) with good accuracy. The uppermost box-shaped spot marked with an asterisk (\*) is manifestly wider at the bottom than at the top, both in the calculated pattern and in the data; and the surrounding spots display the expected profiles.

#### Acknowledgments

This work was carried out at the Research School of Chemistry at the Australian National University. The authors thank the Disordered Materials Group for sponsoring this work; and in particular Aidan Heerdegen, for help with the experimental work and in extracting and post-processing the data; and Richard Welberry, for assistance with the data collection.

#### References

- [1] T.R. Welberry, *Diffuse X-ray Scattering and Models of Disorder* (Oxford University Press Inc., New York, 2004).
- [2] T.R. Welberry, D.J. Goossens, A.P. Heerdegen and P.L. Lee, *Z. Kristallogr.* **220** 1052 (2005).
- [3] L.K. Hansen, G.L. Perlovich and A. Bauer-Brandl, *Acta Cryst.* **E59** 1357 (2003).
- [4] N. Metropolis, A.W. Rosenbluth, M.N. Rosenbluth, A.H. Teller and E.J. Teller, *Chem. Phys.* **21(6)** 1087 (1953).
- [5] D.J. Goossens, A.P. Heerdegen, T.R. Welberry, and A.G. Beasley, unpublished work.